Transactions of the Korean Nuclear Society Autumn Meeting
Gyeongju, Korea, October 28-30, 2015

Numerical Study on POSRV Leak Detection

Yong Sang Ko*, Se Jin Baik, Yoon Jae Choe, Seok Jeong Yune, Eun Kee Kim
KEPCO Engineering & Construction Company, 989-113, Daedeokdaero Yuseong-gu, Daejeon
**Corresponding author: ysko@kepco-enc.com*

1. Introduction

Four pressurizer Pilot Operated Safety Relief Valves (POSRVs) are adopted in Advanced Power Reactor 1400 (APR1400) for providing the overpressure protection function. Each POSRV consists of a Main Valve (MV), two Spring-Loaded Pilot Valve (SLPV) assemblies and Motor Operated Pilot Valves (MOPV). The SLPV acts as a Reactor Coolant Pressure Boundary (RCPB) isolator in the closed position during the normal operation, but it opens automatically when the system pressure increases to its set pressure. The MV opens as the pressure chamber is discharged via the SLPV opening. POSRV can be opened manually by actuating MOPVs. A schematic diagram of the POSRV is shown in Figure 1.

The POSRVs shall be closed tightly to maintain the integrity of RCPB during the normal operation. Leakage through the RCPB is limited extremely. Each POSRV has several discharge lines for MV and auxiliary valves. Temperature instruments are installed on each discharge lines for leakage detection.

In this study, Computational Fluid Dynamics (CFD) analyses using FLUENT are conducted to evaluate the temperature measurement for POSRV leakage detection.

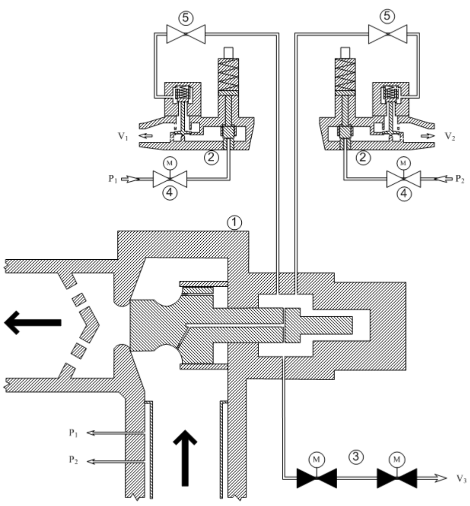

Figure 1. POSRV Schematic Diagram

2. Numerical Analyses

This study analyzes steady state heat transfer phenomena of POSRV in which no-leakage and leakage cases from each valve to discharge lines and different containment temperature are considered. The pressurizer (PZR) is maintained at a pressure of 158.2 kg/cm^2a and a temperature of 345 ℃ for no-leakage and leakage cases. It is assumed that the body temperatures of MV, SLPVs and MOIVs are same as temperature of PZR because all valves are insulated. But the discharge lines of those valves are not insulated. This means that the valve disc surface and leakage temperatures are same as temperature of PZR. The heat transfer from the discharge line to the containment building is considered for both cases.

Churchill and Chu equation [1] is used to calculate the heat transfer coefficient in discharge line. The Churchill and Chu equation is as follows:

$$\mathrm{Nu} = 0.60 + \frac{0.670\mathrm{Ra}^{1/4}}{\left[1+\left(0.492/\mathrm{Pr}\right)^{9/16}\right]^{4/9}} \tag{1}$$

$$\mathrm{h} = \frac{\mathrm{Nu}\times \mathrm{k}}{\mathrm{D_h}} \tag{2}$$

$$\mathrm{Ra} = \frac{g\beta\left(\mathrm{T_h} - \mathrm{T_\infty}\right)\mathrm{D_h}^3}{\nu\alpha} \tag{3}$$

where, Pr, k, D_h, g, β, T_h, T_∞, ν and α represent the Prandtl number, thermal conductivity, hydraulic diameter, gravity, thermal expansion coefficient, hot coolant temperature, containment temperature, dynamic viscosity and thermal diffusivity, respectively. Eq. (2) is the heat transfer coefficient on discharge line. The full buoyancy model is used in this study with variations of air, water-vapor and water-liquid properties due to temperature variation and atmospheric pressure on each discharge line. The steady state analyses are applied to both cases because it is assumed that the leak rate from each valve to discharge line is constant.

The governing equations for no-leakage case for analyzing the conduction and heat loss effects are expressed as:

· Continuity:

$$\nabla \bullet \left(\rho\vec{v}\right) = 0 \tag{4}$$

· Momentum:

$$\nabla \bullet (\rho \vec{v}\vec{v}) = -\nabla p + \nabla[\mu(\nabla \vec{v})] + \rho \vec{g} + \vec{F} \quad (5)$$

· Energy:

$$\nabla \bullet [\vec{v}(\rho E + p)] = \nabla[k(\nabla T)] \quad (6)$$

The discharge line is filled with air before leakage occurs. When leakage occurs, mixture (water-vapor and water-liquid) at high pressure and temperature from each valve flows into the discharge line. It is assumed to be isenthalpic expansion process. Figure 2 is the temperature and enthalpy diagram of water. As shown in Figure 2, the mixture at 158.2 kg/cm^{2}a and 345 ℃ is changed to one at the atmospheric and 100 ℃. In that case, the quality of the mixture is 0.9654 and it is approximated to be 1 (only water-vapor). In this study a three-phase model (air, water-vapor and water-liquid) is used to simulate this phenomenon. Also, the Lee's model [2] is used to calculate condensation from water-vapor to water-liquid. The governing equations for leakage are as follows:

· Continuity:

$$\nabla \bullet (\alpha_a \rho_a \vec{v}_a) = 0 \ \text{[Air phase]} \quad (7)$$

$$\nabla \bullet (\alpha_v \rho_v \vec{v}_v) = -m_{v \to l} \ \text{[Water-vapor phase]} \quad (8)$$

$$\nabla \bullet (\alpha_l \rho_l \vec{v}_l) == m_{v \to l} \ \text{[Water-liquid phase]} \quad (9)$$

· Momentum:

$$\nabla \bullet (\rho_m \vec{v}_m \vec{v}_m) = -\nabla p + \nabla[\mu_m(\nabla \vec{v}_m + \nabla \vec{v}_m^T)] + \rho_m \vec{g} + \vec{F} \quad (10)$$

· Energy:

$$\nabla \bullet \sum_{k=1}^{n} [\alpha_k \vec{v}_k (\rho_k E_k + p)] = \nabla[k_{eff}(\nabla T)] \quad (11)$$

In the above equations, α_a, α_v and α_l represent volume fractions of air, water-vapor and water-liquid. $m_{v \to l}$, ρ_m, $\vec{v}_m$, μ_m and k_{eff} are defined as:

$$m_{v \to l} = 0.1 \times \alpha_l \times \rho_l \times \frac{(T_s \quad T_v)}{T_s} \quad [T_v \le 100℃]$$
$$= 0 \quad [T_v \succ 100℃] \quad (12)$$

$$\rho_m = \sum_{k=1}^{n} \alpha_k \rho_k \quad (13)$$

$$\vec{v}_m = \frac{\sum_{k=1}^{n} \alpha_k \rho_k \vec{v}_k}{\rho_m} \quad (14)$$

$$\mu_m = \sum_{k=1}^{n} \alpha_k \mu_k \quad (15)$$

$$k_{eff} = \sum_{k=1}^{n} \alpha_k k_k \quad (16)$$

The Shear Stress Transport (SST) turbulent model is applied to calculate the turbulent multiphase flow [3, 4].

In this study, it is assumed that the leakage of 0.1 gpm from one valve. Multiple leakages from two or more valves are not considered. The leakage is determined by one-tenth of the unidentified leakage of 1 gpm. The velocities of leakage are determined by dividing discharge line area as the saturated steam at the piping connection points. The containment temperature is listed in Table 1.

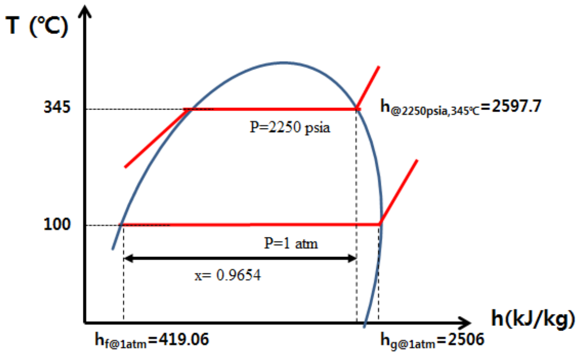

Figure 2. Temperature and Enthalpy Diagram for Water

Figure 3 and Table 1 show the discharge line layout for analyses and the detailed boundary conditions, respectively. Figure 3 presents the discharge line arrangement for each. h_1, h_2 and h_3 indicate the heat transfer coefficients of MV, MOPVs and SLPVs.

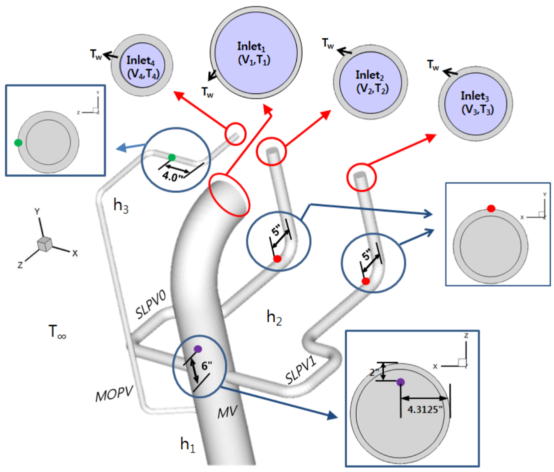

* Dot : Location of Temperature Detector

Figure 3. Discharge Arrangement

Table 1. Boundary Conditions

CASE	Leakage at 345 ℃				T∞ (℃)
	MV	SLPV0	SLPV1	MOPV	
1-1	No				20
1-2	Yes	No	No	No	
1-3	No	Yes	No	No	
1-4	No	No	Yes	No	
1-5	No	No	No	Yes	
2-1	No				30
3-1	No				45
3-2	Yes	No	No	No	
3-3	No	Yes	No	No	
3-4	No	No	Yes	No	
3-5	No	No	No	Yes	
4-1	No				50

3. Results and Discussion

3.1 No-leakage Cases

Figure 4 shows the temperature distributions for no-leakage cases.

The detector temperature is similar to the containment temperature at the downstream of the first bend of each discharge line. The temperature gradient is gentle in the discharge line of MV compared with other piping. That is because the lowest heat transfer coefficient is imposed on the discharge line of the MV.

The temperature in the discharge line for no-leakage cases is 3~4 ℃ greater than the containment temperature.

3.2 Leakage Cases

Figure 5 shows the temperature distributions for leakage cases.

The temperature on the discharge line of MOPV is not significantly affected by leakage from MV, SLPV0 or SLPV1. Also, leakage from MOPV or MV does not have a significant effect on temperature of the discharge line of SLPV0 and SLPV1. In the contrary, any valve leakage causes increase in the temperature on the discharge line of MV. That is because the connecting point of any pilot valve discharge line is close to the temperature sensor in the MV discharge line.

Since this study considers only a fixed leakage flow rate of 0.1 gpm, all leakage cases have a similar maximum temperature and discharge line temperature distributions for MV.

As shown in Table 2, temperature rises due to leakage are 28℃ greater than the containment temperature.

Table 2. Analysis Results

CASE	Temperature Analyzed (℃)				ΔT to T_∞ ℃
	MV	SLPV0	SLPV1	MOPV	
1-1	23.86	20.27	20.28	22.91	< 4
1-2	100.18	20.72	20.72	25.53	+ 80.18
1-3	87.53	59.59	34.43	24.80	+ 39.59
1-4	87.38	34.35	59.64	24.53	+ 39.64
1-5	86.85	36.75	36.73	76.52	+ 56.52
2-1	33.74	30.29	30.29	32.98	< 4
3-1	46.69	45.12	45.12	47.72	< 3
3-2	100.65	45.26	45.26	48.85	+ 55.65
3-3	91.47	73.79	54.53	48.98	+ 28.79
3-4	91.89	54.53	73.84	49.09	+ 28.84
3-5	88.48	53.58	53.61	86.76	+ 41.76
4-1	52.03	50.00	50.00	52.60	< 3

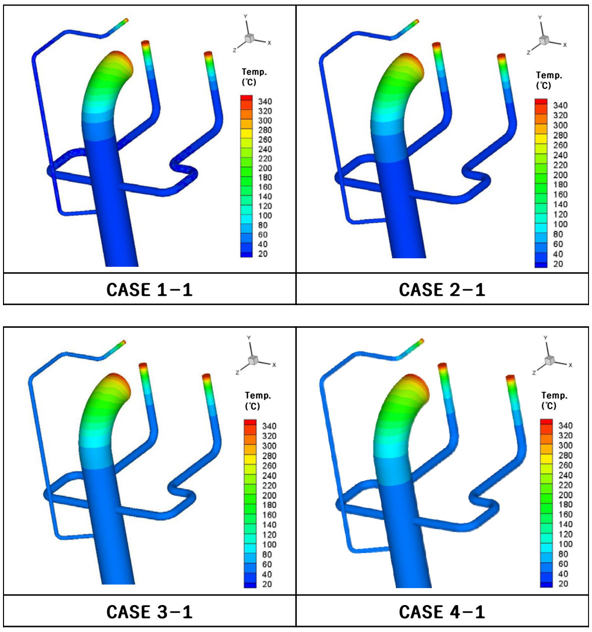

Figure 4. Temperature Distributions for No-Leakage Cases

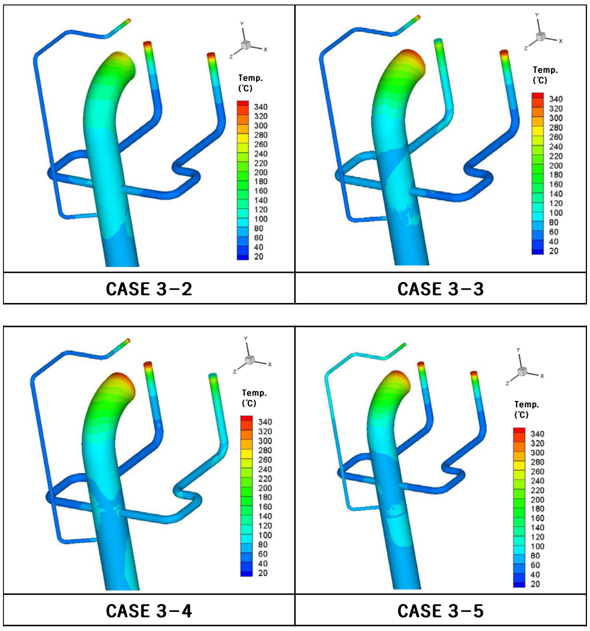

Figure 5. Temperature Distributions for Leakage Cases

4. Conclusions

The followings are concluded from this study:

1) The determined temperature measuring points are adequate for effective leak detection, which are at the downstream of the first bend of each discharge line as close as to the discharge nozzle.
2) The alarm set point for detecting a leak is adequate and can be determined with considering the analysis results.
3) The temperature rise is sufficiently high to detect a small leakage.
4) The temperature sensing method is appropriate for finding a valve leakage.

This study shows that the selected temperature measuring locations on the discharge lines of MV, MOPV, SLPV0 and SLPV1 are adequate for POSRV leakage detection. The analyzed temperature can be used as an alarm setpoint for leakage detection.

REFERENCES

[1] Introduction to Heat Transfer, 5th Edition, Wiley, Incorpera et al.
[2] W.H. Lee, A Pressure Iteration Scheme for Two-Phase Flow Modeling, Technical Report LA-UR 79-975, Los Alamos Scientific Laboratory, Los Alamos, New Mexico, 1979.
[3] A. Dehbi, F. Janasz and B. Bell, Prediction of Steam Condensation in the Presence of Noncondensable Gases using CFD- based Approach, Nuclear Engineering and Design, Vol. 258, pp. 190-210, 2013.
[4] G. Zchaeck, T. Frank and A.D. Burns, CFD Modeling and Validation of Wall Condensation in the Presence of Non-condensable Gases, Nuclear Engineering and Design, Vol. 279, pp.137-146. 2014.